Axial Load Collapse of Reinforced Concrete Columns with Light Transverse Reinforcement

Javad Yadegari[1], Omid Bahar[2*], and Mohammad Khanmohammadi[3]

1. Ph.D. Candidate of Structural Earthquake Engineering, IIEES, Tehran, Iran
2. Assistant Professor, Structural Engineering Research Center, IIEES, Tehran, Iran,
* Corresponding Author; email: omidbahar@iiees.ac.ir
3. Assistant Professor, Department of Civil Engineering, Faculty of Engineering, University of Tehran, Tehran, Iran

ABSTRACT

To assess collapse risk of the older reinforced concrete buildings in Iran, six 1/2-scale concrete columns were tested under Quasi-static cyclic loading, simulating earthquake actions along with constant axial forces. Based on the test results, cracking patterns, hysteretic response, shear strength and drift ratio at axial failure of each specimen are presented. Two different failure modes of columns are recognized. The first mode is S-shaped failure pattern, and the second mode is related to a mushroom failure mode. The latter was developed by crushing of the concrete and lacking of longitudinal reinforcing bars. The mushroom failure mode is expected where the axial force is reasonably large. Experimental results of test specimen are compared with ASCE/SEI 41-06 analytical models. It is found that shear strength of columns is estimated reasonably well by ASCE/SEI 41-06 flexure and shear models. However, the predicted ultimate displacement is too conservative and ASCE/SEI 41-06 does not properly predicted failure mechanism of columns.

1. Introduction

There are a large number of reinforced concrete buildings in Iran and around the world that do not satisfy the special seismic detailing requirements [1]. These buildings are built prior to the introduction of modern seismic codes. Even today, in Iran and many other developing countries, reinforced concrete structures are being designed and built without essential seismic details. Recent earthquakes in Iran have caused widespread damage to reinforced concrete structures with poor seismic design and construction practice [2-4].

Post-earthquake investigations have indicated that failures of columns are the primary cause in the reinforced concrete building collapses [5]. These failures are mainly due to non-seismic details such as widely spaced and poorly anchored transverse reinforcement. Columns with these deficiencies may not have sufficient shear strength, and widely spaced transverse reinforcement could not provide good confinement to the core concrete. These columns may experience formation of critical inclined cracks followed by the loss of lateral-load capacity called shear failure. Lateral-load failure may lead to axial load failure, which then becomes the direct trigger for building collapse.

There are extensive research studies of ductile

reinforced concrete columns throughout past decades [1, 6, 7, 8]. A summary of 107 cyclic lateral load tests on rectangular reinforced concrete columns are collected by Taylor et al. [9]. However, relatively few studies of reinforced concrete columns with non-seismic details have been carried out up to the point of axial failure [10-17]. Due to limited number of experimental studies, failure and collapse mechanism of columns with light transverse reinforcement is not fully understood.

In order to attain a better understanding of the collapse mechanisms of the columns with light transverse reinforcement, an experimental study was conducted at the structural laboratory of the International Institute of Earthquake Engineering and Seismology (IIEES). The test consists of six half-scale reinforced concrete columns that were subjected simultaneously to axial load and quasi-static cyclic lateral load to the point of axial failure. Five out of six columns details were representative of columns used in buildings not designed for seismic loading. Such buildings usually have a wide-spaced transverse reinforcement and 90-degree hooks. One column designed according to the modern seismic design codes.

2. Experimental Program

2.1. Test Specimens

Six ½-scale rectangular section columns were designed and tested up to the point of axial failure. Of those, five column specimens were designed to represent a prototype of the non-ductile reinforced concrete columns. The sixth column was designed according to ACI 318-08 [18] seismic provisions and will be called standard specimen.

Axial loads, main bar ratio and transverse reinforcement ratio were test variables. All specimens had a length of 1400 mm and cross section dimension of 200×300 mm. The longitudinal reinforcement consisted of eight bars. Three specimens were reinforced with Φ10 and two specimens with Φ12 (longitudinal reinforcing ratio of 1.05% and 1.51% respectively). In all cases, Φ6 bars were used as a transverse reinforcement.

All five non-ductile specimens had transverse reinforcement consisting of closed hoops with 90 bend. In three cases, they were spaced 150 mm apart, and in two cases, they were spaced 100 mm. In the standard specimen, cross ties were used as well as closed hoops, and both had standard 135 hooks. The concrete cover was 20 mm. Compressive strength of the concrete was measured on the day of the test. Specimen structural properties are listed in Table (1) and arrangement of reinforcement and sectional view are given in Figure (1).

3. Test Setup and Procedure

The applied loading setup and apparatus are illustrated in Figure (2). The system was designed to make sure that level of lateral load was exactly at the level of inflection point of the column. A vertical actuator at one side of the column and a vertical rod at the other side were used to provide axial load. Actuator applied constant force through the test. The rod was equipped with strain gauge that measured its axial load during the test. At the beginning, rod and actuator had equal forces.

During each test, upper joint of column rotated slightly and rod force changed. The amount of upper joint rotation and rod force were recorded. A reversible horizontal load was applied to the top of the column, using a 25 ton capacity actuator, which was mounted on a reaction frame. The actuator was pinned at both ends to allow rotation during the test.

Table 1. Basic property of column specimens.

Spec.	$P(ton)$	$f'_c(kg/cm^2)$	$\dfrac{P}{f'_c A_g}$	$f_{yl}(kg/cm^2)$	$f_{yt}(kg/cm^2)$	ρ_h	ρ_v
S1	30	146	0.34	3400	2800	0.0057	0.010
S2	30	146	0.34	3400	2800	0.0019	0.010
S3	30	220	0.23	3100	2800	0.0019	0.013
S4	50	220	0.38	3100	2800	0.0019	0.013
S5	30	264	0.19	3400	2800	0.0028	0.010
S6	50	264	0.32	3400	2800	0.0028	0.010

Notation: ρ_h is the longitudinal reinforcement ratio. ρ_v is the lateral reinforcement (A_{sh}/bs). A_{sh} is the total area of transverse reinforcement; s is the tie spacing; and b is the column section width.
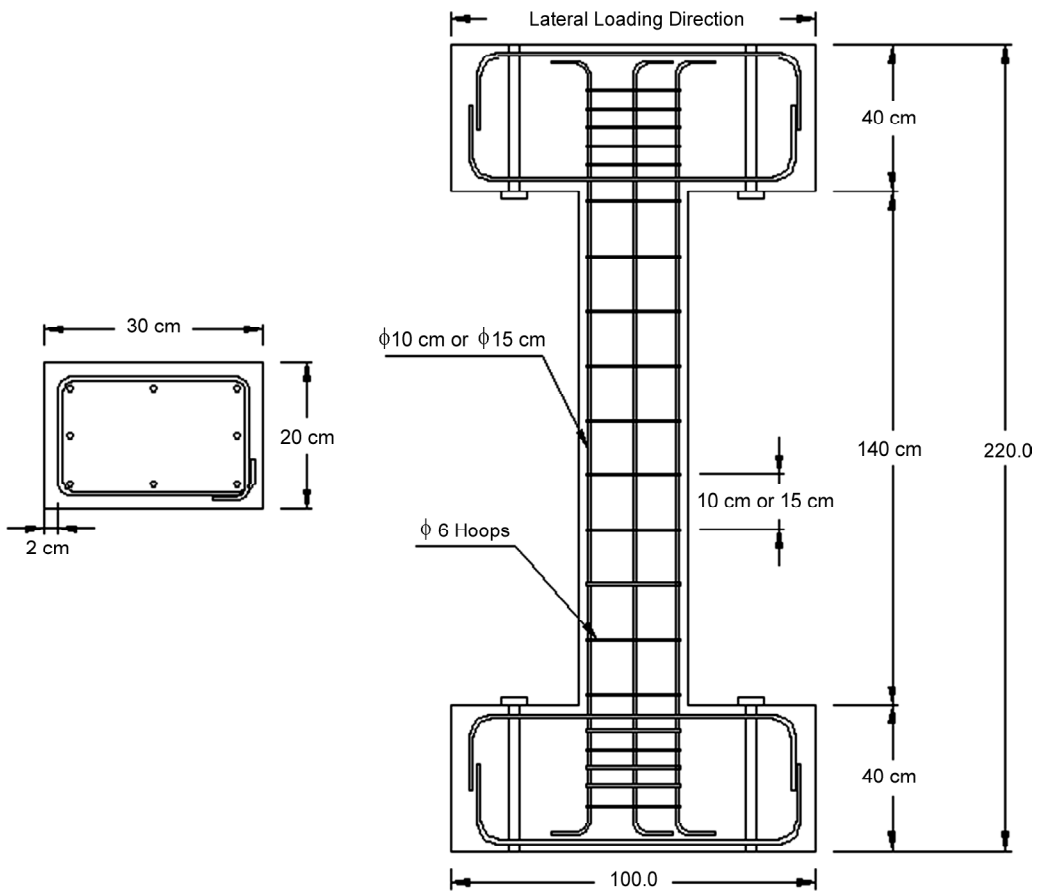
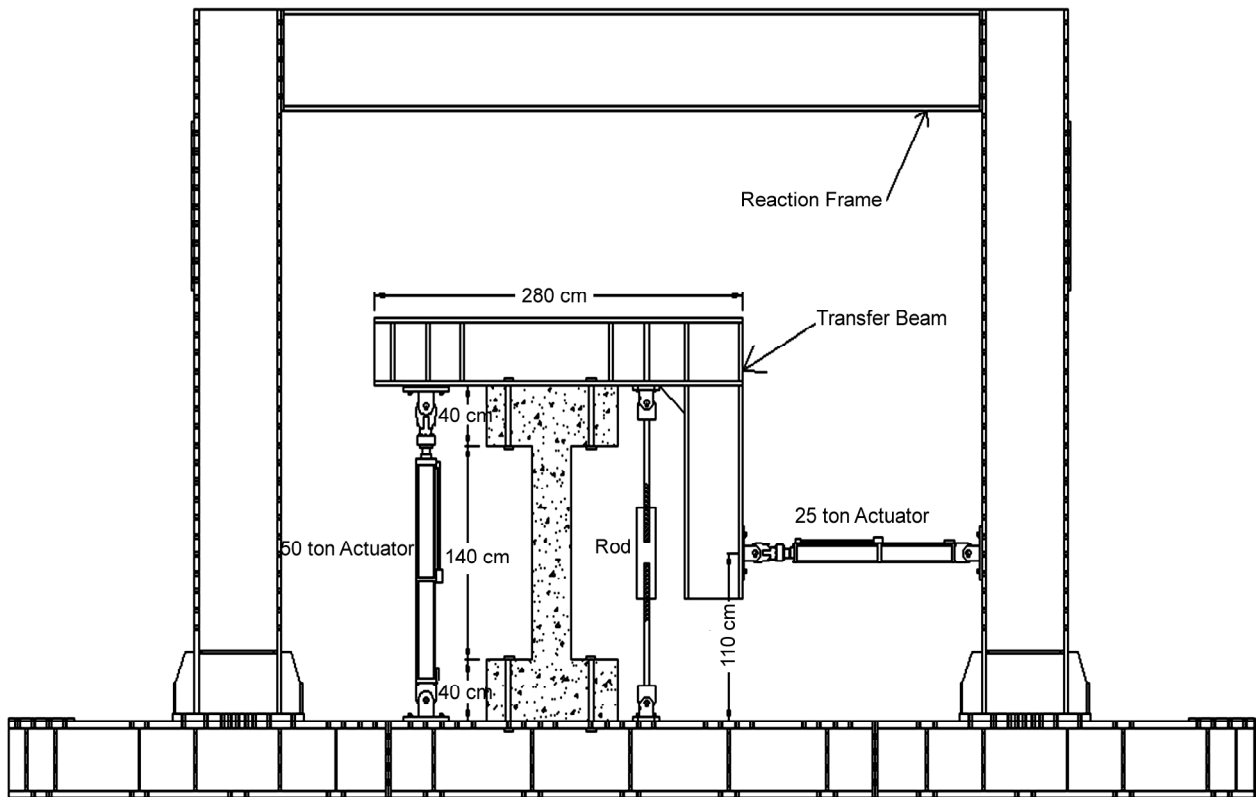**Figure 1.** Typical Detail of Specimens.

Figure 2. Loading apparatus and details of test setup.

The base of the column was fixed to a strong floor by four post-tensioned bolts.

The specimens were tested under the combination of a constant vertical force and a cyclic horizontal force. At first, the axial load was applied to the specimens until the designated level was achieved. Then the lateral load was applied cyclically through the horizontal actuator in a quasi-static fashion as shown in Figure (2). The loading procedure consisting of displacement-controlled steps is illustrated in Figure (3).
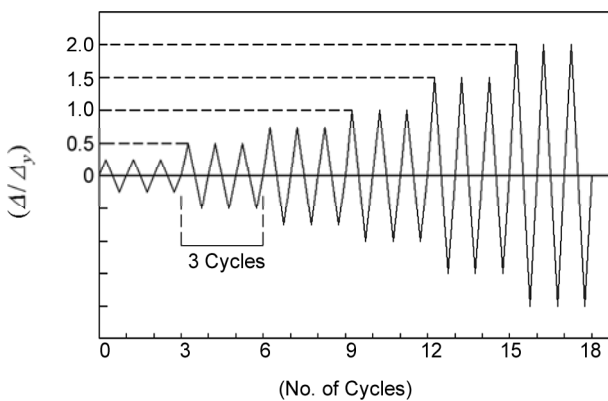

Figure 3. Lateral loading procedure.

The prescribed lateral displacement history was a function of the yield displacement. The yield displacement is sum of three components: flexure, slip and shear. Displacement due to flexure was obtained assuming the curvature varied linearly from the yield curvature at the ends to zero at mid height, yielding a value of 3.5 mm. The contribution of bar slip and shear distortion at the yield load were calculated as 3 mm and 0.3 mm, respectively [19]. Based on these calculations, during the tests, a yield displacement D_y of 8 mm was used for the lateral displacement histories. The displacement history was applied initially with three cycles each at one fourth and one half of the calculated yield displacement. Once the yield displacement was reached, the amplitude of the displacement cycles was increased incrementally, i.e., three cycles each at D_y, $1.5D_y$, $2D_y$, $3D_y$, etc., until the specimen failed.

Within each test, 22 data channels were recorded at regular intervals. 16 strain gauges and six LVDTs (Linear Voltage Displacement Transducer) were used. Four strain gauges were placed on the rod to observe and control the axial load changes.

4. Experimental Results and Discussion

4.1. Test Observation

During the tests, all important signs of deterioration such as cracking, spalling, yielding and buckling were recorded. Failure patterns differed for the different test specimens, as follows:

4.1.1. Specimen 1

Flexural cracks appeared at top and bottom of the columns at the drift of 0.8%. Inclined cracks emerged at the drift of 1.1% and concentrated in ¼ lengths of columns at both side under increasing displacement. Spalling of cover concrete was started at the drift of 2.3% and significant spalling was occurred at the drift ratio of 3.6%. Longitudinal reinforcements buckled at the drift of 4.6%. Lateral resistance started to drop at the drift of 4%. Continued cycling caused additional damage and loss of resistance. Test ended at the drift ratio of 5.7%, by which time lateral resistance had degraded effectively to zero but the column continued to support axial load. Figure (4) shows specimen 1 at the end of the test.

4.1.2. Specimen 2

Initial lateral stiffness of this specimen and specimen 1 was apparently the same owing to axial load. At the drift of 3.4% spalling of concrete was started and continued by buckling of the longitudinal bars. Lateral and axial failure occurred suddenly with the occurrence of a steep diagonal crack and apparent concrete crushing near the top of the column. Figure (5) shows specimen 2 at the end of the test.

4.1.3. Specimen 3

Flexural cracks became visible at the drift ratio of 1.1% and then flexural-shear cracks appeared at the drift of 2.9%. At the drift ratio of 3.4% spalling of the cover concrete was started. Longitudinal bars buckled at the drift of 4.6%. The test stopped at the drift ratio of 5.1% when substantial decrease in lateral resistance of column was observed. Figure (6) shows specimen 3 at the end of the test.

4.1.4. Specimen 4

Initial lateral stiffness of specimen 4 was

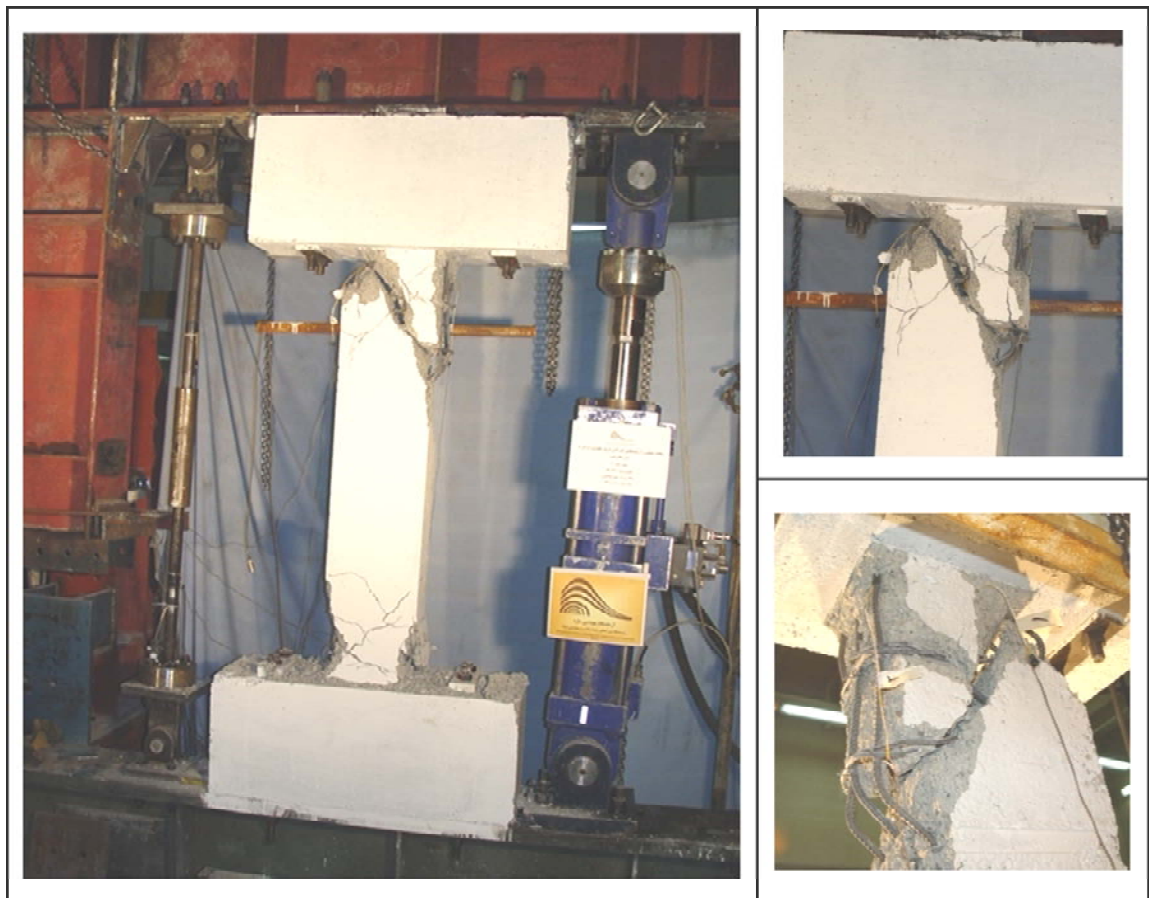**Figure 4.** Crack pattern and axial failure in column S1.

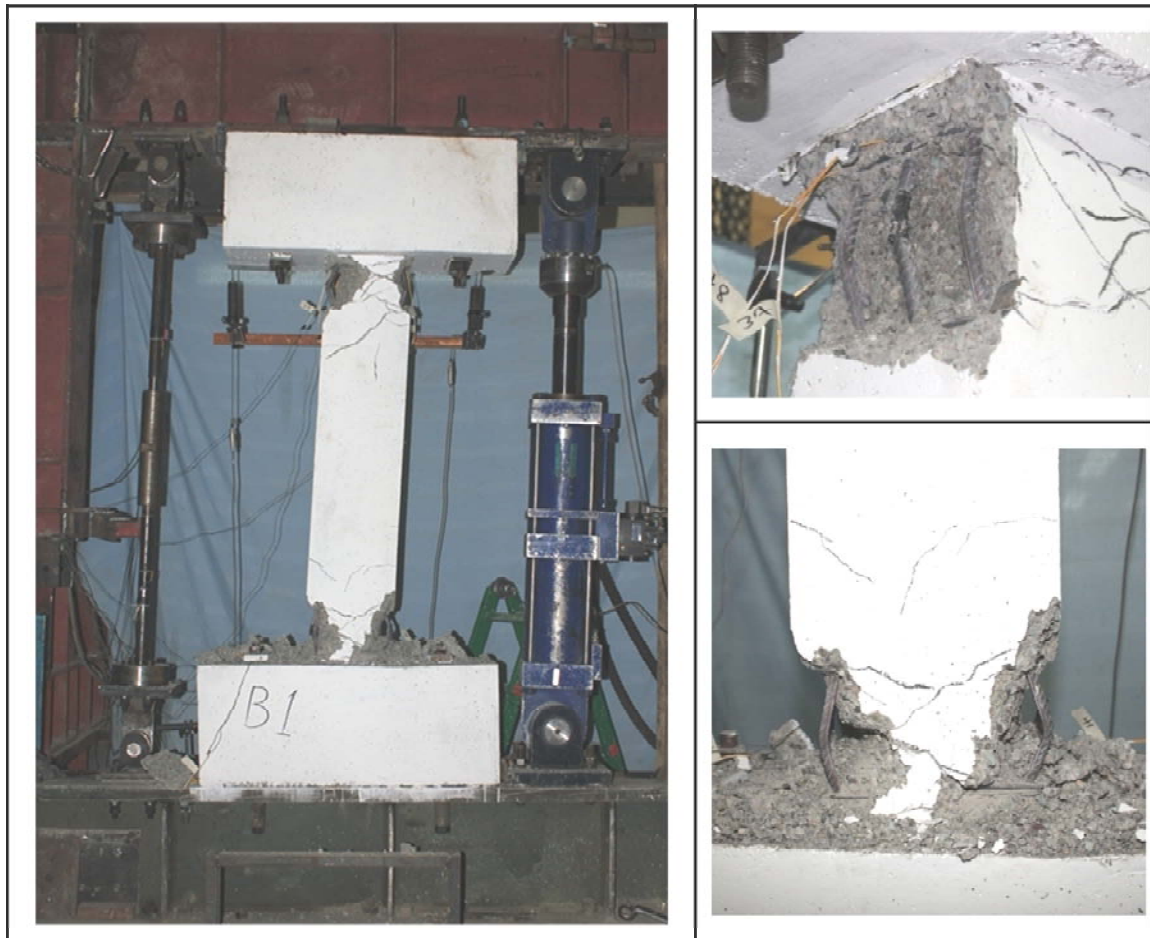**Figure 5.** Crack pattern and axial failure in column S2.

Figure 6. Crack pattern and axial failure in column S3.

obviously higher than that of specimen 3, owing to higher axial load. At the drift ratio of 2.3% main bars buckled and at the drift ratio of 2.9% column collapsed suddenly by crushing of concrete near the bottom of the column. Figure (7) shows specimen 4 at the end of the test.

4.1.5. Specimen 5

Flexural cracks initially appeared at the drift of 0.9% and then flexural-shear cracks became visible at the drift ratio of 2.3%. Main bars buckling and cover concrete spalling started at the drift of 3.4%. As the test continued, lateral resistance apparently decreased and column lost its gravity load carrying capacity at the drift of 5.1%. Figure (8) shows specimen 5 at the end of the test.

4.1.6. Specimen 6

Specimen 6 and 5 were exactly identical in details and properties. Initial lateral stiffness of specimen 6 was higher than that of specimen 5, owing to higher

axial load. At the drift ratio of 2.9%, significant spalling of cover concrete occurred. At the drift of 4%, column lost its gravity load carry capacity and axial failure happened. Figure (9) shows specimen 6 at the end of the test.

5. Moment and Shear Strength

The nominal moment strength of column specimens, M_n was calculated for measured concrete compression and steel yield strengths using the procedures outlined in the ACI318-08 [18]. The maximum plastic moment, M_p was calculated using moment-curvature analysis with measured material properties. Mander confined concrete model [20] was used for concrete stress-strain relationship. The steel stress-strain relation included strain hardening based on tests.

According to ACI 318-08 [18] suggestion, it is possible to increase M_n by 25% to calculate M_p assuming that the longitudinal steel strength can be equal to $1.25 f_y$ at ultimate. However, moment
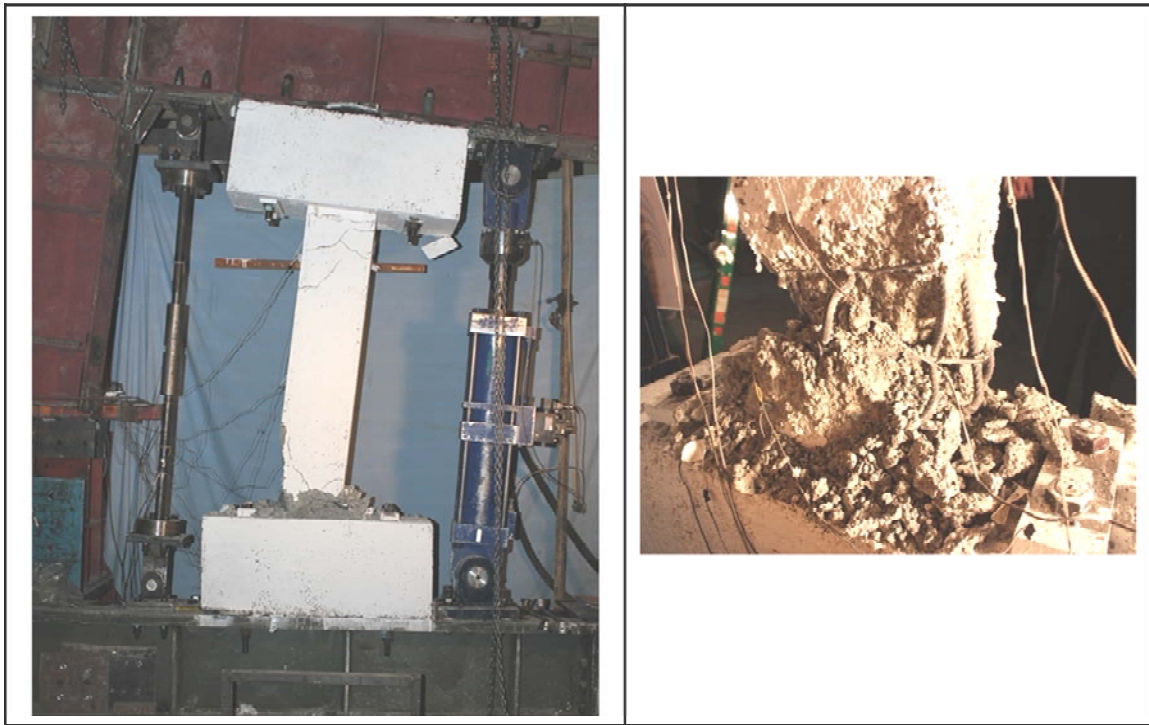
Figure 7. Crack pattern and axial failure in column S4.

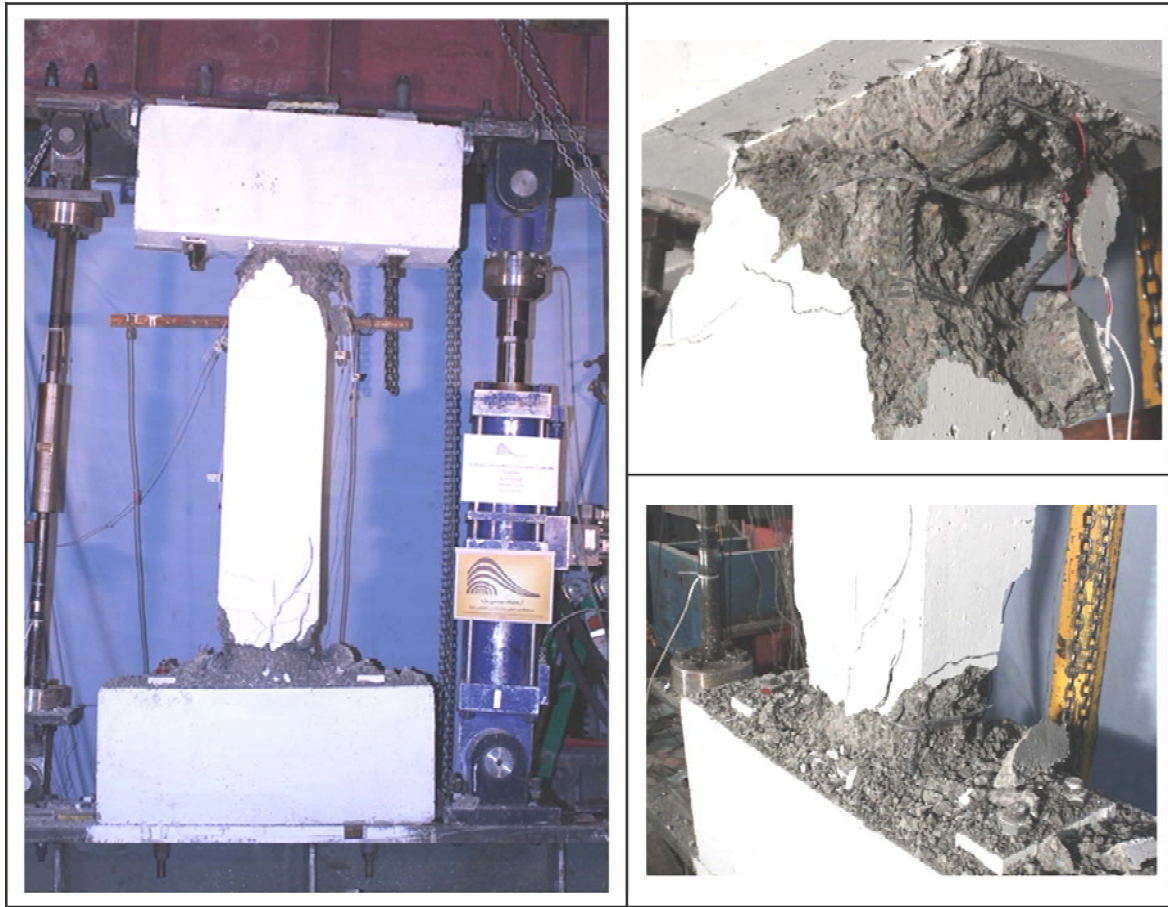**Figure 8.** Crack pattern and axial failure in column S3.

Figure 9. Crack pattern and axial failure in column S6.

curvature analysis showed that the difference between ACI nominal moment strength M_n and plastic moment M_p was very small. As shown in Table (2), M_p can be obtained by justifying a 10% increase in M_n.

The nominal shear strength of the columns was calculated using ACI 318-08 and ASCE 41-06 [21] procedure. For columns satisfying the detailing and proportioning requirements of Chapter 21 of ACI 318, the shear strength equation of ACI 318 can be used [21]. For columns with light transverse reinforcement shear strength was calculated according to ASCE 41-06 equation. Shear corres-

ponding to plastic moment strength was calculated as $V_p = 2M_p/L_n$, where L_n = column clear height. Calculated and measured shear strength of column specimens are shown in Table (3).

Failure mode of column can be expected based on ratio of V_p to V_n. Specimens S2 to S6 are columns with non-seismic details and light transverse reinforcements. Ratio of V_p to V_n in these columns is ranging between 0.74 and 0.9; therefore, the specimens were expected to fail in shear prior to yielding of the flexural reinforcement [22]. With the

Table 2. Measured and calculated moment strengths.

	M_n (Ton-m)	M_P (Ton-m)	M_{test} (Ton-m)	M_{test}/M_n	M_{test}/M_P
S1	4.60	5.10	6.00	1.30	1.18
S2	4.61	4.94	6.20	1.34	1.26
S3	5.70	6.60	6.93	1.22	1.05
S4	6.20	6.80	8.40	1.35	1.24
S5	5.80	6.50	6.93	1.19	1.07
S6	6.60	7.47	8.75	1.33	1.17

Table 3. Measured and calculated shear strengths.

	$V_{n,ACI}$ (Ton)	$V_{n,ASCE41}$ (Ton)	V_{test} (Ton)	V_P	$V_{test}/V_{n,ASCE41}$	V_{test}/V_P	V_p/V_n
S1	13.2	15.2	8.6	7.29	0.57	1.18	0.55
S2	7.5	9.5	8.8	7.06	0.93	1.25	0.74
S3	8.6	10.5	9.9	9.43	0.94	1.05	0.90
S4	9.6	12	12	9.71	1.00	1.24	0.81
S5	10.5	12.4	9.9	9.29	0.80	1.07	0.75
S6	11.6	14	12.5	10.67	0.89	1.17	0.76

exception of column S2, shear failure mode was not observed in the tests.

6. Hysteretic Responses

Hysteretic responses for all six specimens as well as the backbone curve for each hysteresis are presented in Figure (10). The degradation of

stiffness and load-carrying capacity was observed in all hysteretic loops during repeated cycles. This degradation is mainly due to the cracking of the concrete, yielding and buckling of the reinforcing bars. The hysteretic loops of the specimens also show pinching effect. Except for the column S4, the axial failure in all columns occurred at a drift ratio
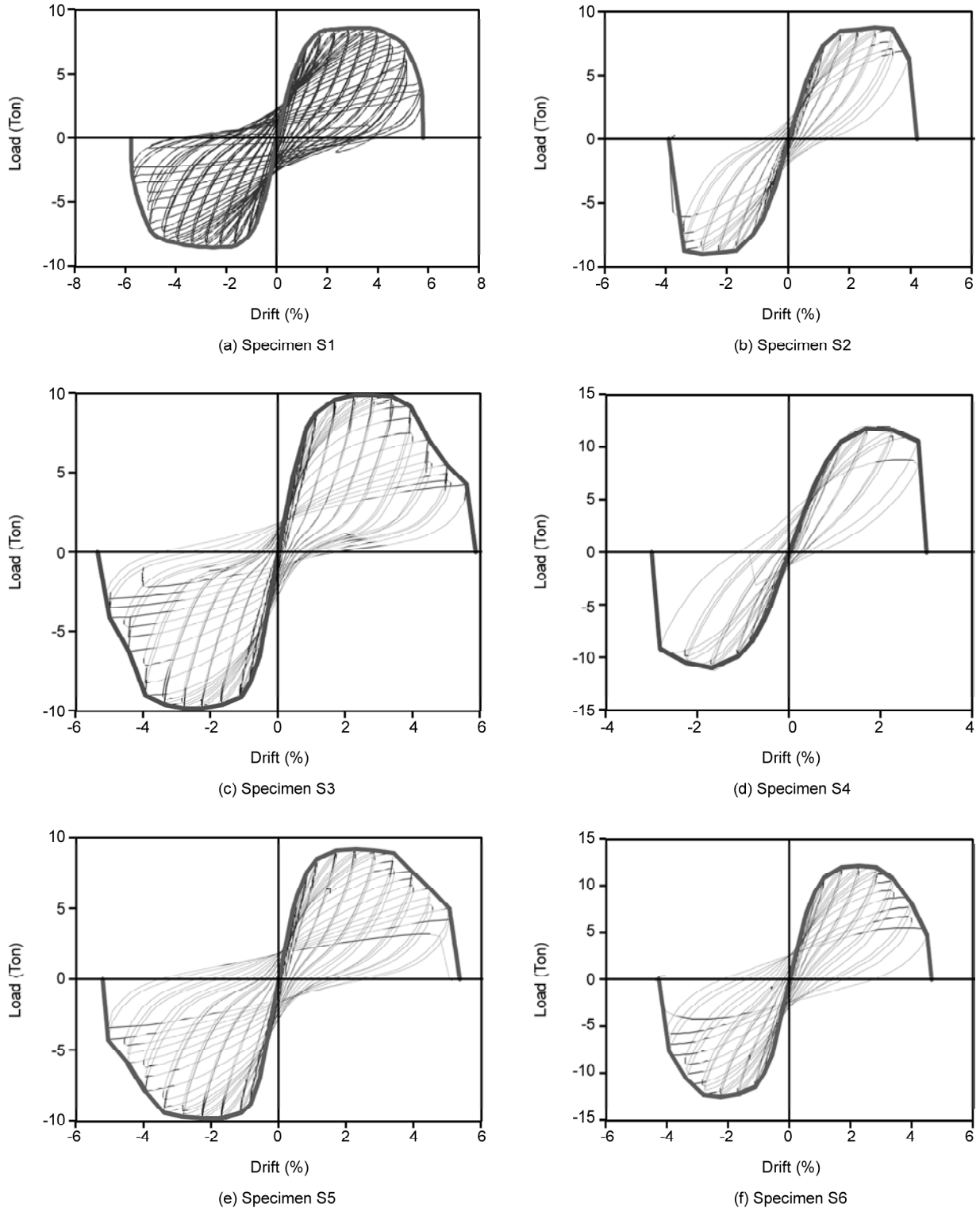

Figure 10. Hysteretic responses of all test specimens.

more than 4%. Axial failure occurred at the drift ratio of 3% in the column S4 mainly due to higher axial load. Despite non-seismic details, hysteretic response of column S2 to S6 shows that they have a considerable ability of energy dissipation.

7. Comparison with ASCE/SEI 41-06

Seismic assessment and rehabilitation of existing buildings are generally performed with aid of ASCE/SEI 41-06 [21] standard. The provision for concrete structures in chapter 6 of ASCE/SEI 41 and its predecessor document, FEMA 356 [23], was basically the same. Figure (11) shows general load-deformation for reinforced concrete columns. Modeling parameters (a, b and c) as well as acceptance criteria for concrete columns are also provided in Tables (6) to (8) of ASCE/SEI 41-06 standard. Load-deformation relationship for a specific column can be generating by using provided guidelines in the ASCE/SEI 41-06 standard.
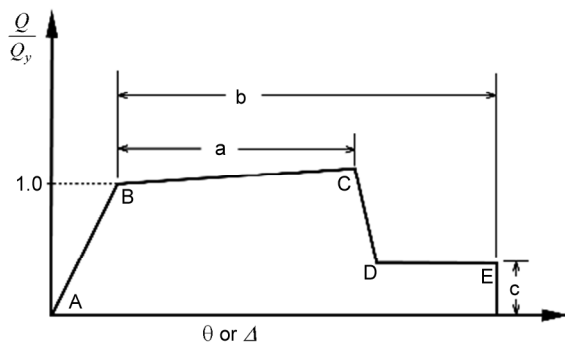

Figure 11. General load and deformation according to ASCE/ SEI 41-06.

In order to generate a load-deformation relationship for a given column as shown in Figure (11), points B, C, D and E need to be determined. Point B is defined by determining initial stiffness, displacement and/or lateral load at yielding. According to ASCE/SEI 41-06, the slope from point B to C can be either zero or 10% of initial slope. In this study, the slope is assumed to be zero. Point C, D and E is determined by calculating plastic hinge rotation angles "a" and "b" as well as residual strength ratio "c". Parameters "a" and "b" depend on axial load, nominal shear stress and reinforcement details are extracted from table 6-8 of ASCE/SEI 41-06. Parameter "c" is equal to 0.2.

The Shear strength of RC column in ASCE/SEI 41-06 is defined by the following equation:

$$V_n = k \frac{A_v f_y d}{s} +$$

$$\lambda k \left(\frac{6\sqrt{f_c'}}{M/_{vd}} \sqrt{1 + \frac{N_u}{6\sqrt{f_c'} A_g}} \right) 0.8 A_g \quad (1)$$

where, $k = 1.0$ in regions where displacement ductility is less than or equal to 2, $k = 0.7$ in regions where displacement ductility is greater than or equal to 6, and varies linearly for displacement ductility between 2 and 6. M and V = moment and shear at section of maximum moment, and the value of M/V_d is limited to $2 \leq a/d \leq 4$. Details explanation of the equation can be found in ASCE/SEI 41-06 [21].

An update to the concrete provision of ASCE/SEI 41-06 was introduced in order to incorporate latest experimental results [22]. Table 6-8 in ASCE/SEI 41-06 is completely updated and replaced with a new table in the proposed provision. Definition of the initial stiffness of concrete columns is also slightly modified.

Comparison of the test specimen envelopes with ASCE/SEI 41-06 flexure and shear models as well as proposed provision of ASCE/SEI are shown in the Figure (12). ASCE/SEI shear model shows good agreement with the experimental results. Flexural model of the proposed provision is less conservative than ASCE/SEI 41-06 flexural model.

8. Conclusion

Six half-scale reinforced concrete columns were tested under gravity and cyclic lateral loads to the point of axial failure. Five specimens represented of non-ductile building columns with light transverse reinforcement. For comparison purpose, one specimen designed according to modern seismic codes.

Axial failure modes of columns could be divided into two different types. In the first mode, an S-shaped failure pattern was observed. In the second mode, a mushroom failure shape was developed by crushing of the concrete and buckling of longitudinal reinforcing bars.

Experimental results of the column specimens were compared with flexural and shear models of ASCE/SEI 41-06 and proposed provision of ASCE/SEI 41-06. The comparisons showed that maximum observed shear strengths of the columns were
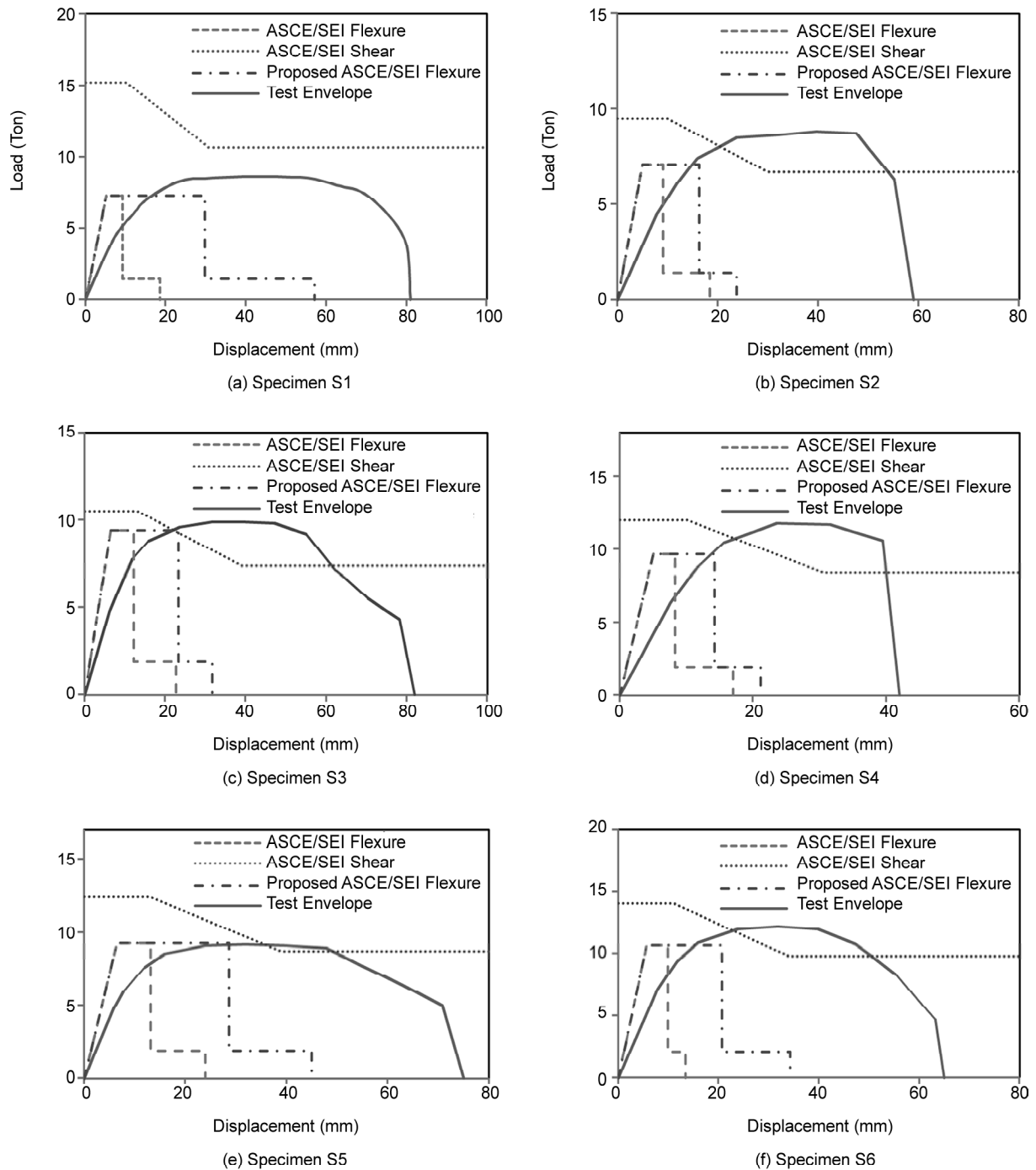
Figure 12. Comparison of the backbone curve of the test specimens with ASCE/SEI model.

predicted relatively accurate using ASCE/SEI 41-06. The initial stiffness was underestimated in both provisions mainly due to slip of longitudinal reinforcement from the beam-column connections. The predicted ultimate displacement was too conservative in ASCE/SEI 41-06. Although ultimate displacement obtained with the proposed provision of ASCE/SEI 41-06 showed an improvement, the results were still rather conservative. Furthermore, it was found that the predicated failure mode was inconsistent with the observed behavior of the columns.

References

1. Marefat, M., Khanmohammadi, M., Bahrani, M., and Goli, A. (2006) Experimental assessment of reinforced concrete columns with deficient seismic details under cyclic load. *Advances in Structural Engineering*, **9**(3), 337-347.

2. Naeim, F. and Ghafory-Ashtiany, M. (2005) *2003 Bam, Iran, Earthquake Reconnaissance Report,* 22. Oakland, CA: Earthquake Engineering Research Institute.

3. Ghalandarzadeh, A., Kavand, A., Bahadori, A., Keyvani, A., and Mousavi, M. (2005) *Reconnaissance Report of Zarand Earthquake of February 2005-Structural and Geotechnical Aspects*. Tehran: Department of Civil Engineering, University of Tehran.

4. Razzaghi, M. and Ghafory-Ashtiany, M. (2012) *A Preliminary Reconnaissance Report on August 11th 2012, Varzaghan-Ahar Twin Earthquakes in NW of Iran*. www.eeri.org.

5. Moehle, J. and Mahin, S. (1991) Observations on the behavior of reinforced concrete building during earthquakes. ACI SP-127, *Earthquake-Resistant Concrete Structures Inelastic Response and Design*, 67-89.

6. Esmaeily, A. and Xiao, X. (2004) Behavior of reinforced concrete columns under variable axial loading. *ACI Structural Journal,* **101**(1), 124-132.

7. Pujol, S. (2002) *Drift Capacity of Reinforced Concrete Columns Subjected to Displacement Reversals*. Ph.D. Thesis, School of Civil Engineering, Purdue University.

8. Saatcioglu, M. and Ozcebe, G. (1989) Response of reinforced concrete columns to simulated seismic Loading. *ACI Structural Journal*, **86**(1), 3-12.

9. Taylor, A., Kuo, C., Wellenius, K., and Chung, D. (1997) *A Summary of 107 Cyclic Lateral Load Tests on Rectangular Reinforced Concrete Columns*. National Institute of Standards and Technology Report NISTIR 5984.

10. Lynn, A.C. (2001) *Seismic Evaluation of Existing Reinforced Concrete Building Columns*. Ph.D. Dissertation. Department of Civil and Environmental Engineering, University of California, Berkeley.

11. Sezen, H. (2002) *Seismic Response and Modeling of Reinforced Concrete Building Columns*. Ph.D. Dissertation, Department of Civil and Environmental Engineering, University of California, Berkeley.

12. Nakamura, T. and Yoshimura, M. (2002) Gravity load collapse of reinforced concrete columns with brittle failure modes. *Journal of Asian Architecture and Building Engineering*, **1**(1), 21-27.

13. Yoshimura, M. and Nakamura, T. (2003) Axial collapse of reinforced concrete short columns. *Toba, Japan: the 4th US-Japan Workshop on Performance-Based Earthquake Engineering Methodology for Reinforced Concrete Building Structures*, 22-24 Oct. 2002, Toba, Japan.

14. Ousalem, H. (2003) *Experimental and Analytical Study on Axial Load Collapse Assessment and Retrofit of Reinforced Concrete Columns*. University of Tokyo, Tokyo.

15. Ngoc Tran, C. (2010) *Experimental and Analytical Studies on the Seismic Behavior of RC Columns*. Ph.D. Thesis, Nanyang Technological University, Singapore.

16. Matchulat, L. (2009) *Mitigation of Collapse Risk in Vulnerable Concrete Buildings*. Lawrence: University of Kansas.

17. Woods, C. (2010) *Mitigation of Collapse Risk in Vulnerable Concrete Buildings*. Lawrence: University of Kansas.

18. ACI Committee 318 (2008) *Building Code Requirements for Structural Concrete and Commentary*. Farmington Hills: American Concrete Institute.

19. Yadegari, J. (2013) *Experimental and Analytical Studies on the Axial Failure of Non-Ductile Reinforced Concrete Columns*. Ph.D. Thesis, International Institute of Earthquake Engineering and Seismology, Iran.

20. Mander, J., Priestley, M., and Park, R. (1988) Theoretical stress-strain model for confined concrete. *Journal of Structural Engineering*, **114**(8), 1804-1826.

21. ASCE/SEI 41 (2007) *Seismic Rehabilitation of Existing Buildings*. Reston, VA: American Society of Civil Engineers.

22. Elwood, K., Matamoros, A., Wallace, J., Lehman, D.E., Heintz, J.A., Mitchell, A.D., Moore, M.A., Valley, M.T., Lowes, L.N., Comartin, C.D., and Moehle, J. (2007) Update to ASCE/SEI 41 concrete provisions. *Earthquake Spectra*, **23**(3), 493-523.

23. FEMA 356 (2000) *Prestandard and Commentary for the Seismic Rehabilitation of Buildings*. Washington D.C., USA: Federal Emergency Management Agency.